Neutron star properties in density-dependent relativistic mean field theory with consideration of an isovector scalar meson

Sha Wang (王莎) and Hong Fei Zhang (张鸿飞)*
School of Nuclear Science and Technology, Lanzhou University, Lanzhou 730000, People's Republic of China

Jian Ming Dong (董建敏)
Research Center for Nuclear Science and Technology, Lanzhou University and Institute of Modern Physics of CAS, Lanzhou 730000, People's Republic of China

(Received 27 May 2014; revised manuscript received 19 September 2014; published 10 November 2014)

Based on the density-dependent relativistic mean field theory, the properties for nuclear matter and neutron stars with the effective interaction DD-MEδ including the isovector scalar channel which disentangle the effects of isovector scalar and isovector vector channels by fitting microscopic calculations. The influences of the isovector scalar δ meson on properties of asymmetric nuclear matter at high densities are discussed in detail. The results support that the isovector scalar channel can soften the equation of state through the effects on the nucleon effective mass and the scalar σ field and impact the behavior of the nuclear matter symmetry energy. Because of the influence on the symmetry energy by the δ meson, a larger proton fraction in neutron stars is predicted by the DD-MEδ calculation, which strongly affects the cooling process of the star. The maximum masses of neutron stars given by the DD-MEδ calculation is $1.97M_{\odot}$ which is in reasonable agreement with PSR J1614 − 2230 ($1.97 \pm 0.04\ M_{\odot}$) and PSR J0348 + 0432 ($2.01 \pm 0.04\ M_{\odot}$). Among all the selected interactions, DD-MEδ gives the smallest radius range. The radius for the 1.4 solar mass neutron star calculated by DD-MEδ is in good agreement with the prediction [Astrophys. J. Lett. **765**, L5 (2013)] according to the resent observations.

DOI: 10.1103/PhysRevC.90.055801 PACS number(s): 21.65.Ef, 21.30.Fe, 21.60.Jz, 26.60.Kp

I. INTRODUCTION

Neutron stars [1], as the natural laboratories to test the properties of hadronic matter under extreme conditions, have been one of the hottest topics both in nuclear physics and astrophysics since Landau first predicted the existence of neutron stars in 1932 [2]. In the investigation of neutron stars, searching for the proper equation of state (EOS) was a long-sought goal and central task. It is known that EOS is very important to describe the properties of neutron stars, for example, EOSs generate unique mass radius (M-R) relations for neutron stars. However, because the poorly constrained many-body interaction at supranuclear densities, there still exists considerable theoretical uncertainty on the EOS [3]. Thus precise and massive modern astronomical observations are especially important in providing constraints for EOS and M-R relation. In the year of 2010, a large pulsar mass of $(1.97 \pm 0.04)M_{\odot}$ was measured using the Shapiro delay for the binary millisecond pulsar J1614 − 2230 [4]. Recently, another two-solar-mass pulsar J0348 + 0432 was determined with high accuracy as 2.01 ± 0.04 solar masses [5]. These two neutron stars are the most massive ones observed precisely by now which demand theoretical models providing a sufficient maximum mass.

In the past several years, there have been several attempts to set constraints on the high-density EOS and M-R relation according to the observations [6–9] or microscopic calculations [10]. Recently new constraints of the mass-radius relation based on recent observations have been proposed [11], and the results imply that many models are inconsistent with the observations.

During recent decades, many successes have been achieved in describing nuclear properties from stable to unstable nuclei in the relativistic energy density functional theory including the relativistic mean field (RMF) and the relativistic Hartree-Fock (RHF) approaches from the covariant structure of theory itself [12–15]. At present, the widely used RMF approach includes the isoscalar scalar channel (σ meson), the isoscalar vector channel (ω meson), and the isovector vector channel (ρ meson), but no isovector scalar channel because fitting the experimental data based on finite nuclei properties does not allow us to distinguish scalar and vector fields in the isovector channels. However, for strongly isospin-asymmetric matter at high densities in neutron stars, neglecting the isovector scalar seems to be improper. In recent years, the importance of the contribution to asymmetric nuclear matter from the isovector scalar δ meson within the RMF model, was stressed [16–18]. Later, researchers introduced the δ meson in the nonlinear RMF model [19–21]. However, a common problem in the widely used RMF is to disentangle the effects of isovector scalar and isovector vector channels by means of nuclear ground-state properties, unless a careful tuning is performed based on selected microscopic calculations [22]. Recently, a new high-precision density functional DD-MEδ is presented which includes the δ meson, with density-dependent meson-nucleon couplings, and which to a large extent based on microscopic *ab initio* calculations in nuclear matter [22]. By the way, although the modern relativistic Hartree-Fock and Hartree-Fock-Bogoliubov models do not include the degree of freedom associated with the δ meson, the Fock terms indeed present substantial contributions to the isovector scalar channel

*zhanghongfei@lzu.edu.cn

that is taken into account by the δ field in the RMF scheme. The direct evidence is that the Fierz transformation of the Fock diagram of ρ-vector coupling results in the isovector scalar component. Such contributions can also be deduced from the localization of the Fock terms of the isovector vector channel [23].

In this paper, the properties for nuclear matter and neutron stars in the framework of the density-dependent relativistic mean field theory with the interaction DD-MEδ are systematically compared to those with the interactions DD-ME2 [24], TW99 [25], and PKDD [26] which neglect the δ meson. The influences of the isovector scalar δ meson on properties of asymmetric nuclear matter at high densities are discussed in detail. The purpose of this work is to investigate the effect of the isovector scalar channel on the EOS as well as the properties of neutron stars. In Sec. II, the equation of state for neutron star matter when considering the isovector scalar meson δ is presented. Then the results and discussions are given in Sec. III. Finally we give a brief summary in Sec. IV.

II. THEORETICAL FRAMEWORK

The effective Lagrangian density described nuclear matter with the nucleon (ψ), two isoscalar mesons (scalar σ, vector ω), and two isovector mesons (scalar δ, vector ρ) as degrees of freedom can be written as

$$\begin{aligned}\mathcal{L} = &\sum_B \bar{\psi}_B[i\gamma^\mu\partial_\mu - (m_B - g_\sigma\sigma - g_\delta\vec{\tau}_B\cdot\vec{\delta}) - g_\omega\gamma^\mu\omega_\mu \\ &- g_\rho\gamma^\mu\vec{\tau}_B\cdot\vec{\rho}_\mu]\psi_B + \frac{1}{2}\partial^\mu\sigma\partial_\mu\sigma - \frac{1}{2}m_\sigma^2\sigma^2 \\ &- \frac{1}{4}\Omega_{\mu\nu}\Omega^{\mu\nu} + \frac{1}{2}m_\omega^2\omega^\mu\omega_\mu + \frac{1}{2}\partial^\mu\vec{\delta}\cdot\partial_\mu\vec{\delta} - \frac{1}{2}m_\delta^2\vec{\delta}^2 \\ &- \frac{1}{4}\vec{R}_{\mu\nu}\cdot\vec{R}^{\mu\nu} + \frac{1}{2}m_\rho^2\vec{\rho}^\mu\cdot\vec{\rho}_\mu, \end{aligned} \tag{1}$$

where the Dirac spinor ψ_B denotes the hadron B with mass m_B and isospin τ_B. The σ, ω, ρ, and δ are the σ-meson field, ω-meson field, ρ-meson field, and δ-meson field, respectively. Their masses are denoted by m_σ, m_ω, m_ρ, and m_δ. The corresponding coupling constants are g_σ, g_ω, g_ρ, and g_δ. The field tensor $\Omega_{\mu\nu}$ and $\vec{R}_{\mu\nu}$ are

$$\Omega_{\mu\nu} = \partial_\mu\omega_\nu - \partial_\nu\omega_\mu, \quad \vec{R}_{\mu\nu} = \partial_\mu\vec{\rho}_\nu - \partial_\nu\vec{\rho}_\mu. \tag{2}$$

The coupling constants of density-dependent RMF theory are denoted by

$$g_i(\rho) = g_i(\rho_0)f_i(x) \quad \text{for} \quad i = \sigma,\omega,\rho,\delta, \tag{3}$$

where ρ_0 is the saturation density of symmetric nuclear matter and $x = \rho/\rho_0$. For the functions $f_i(x)$, we follow Ref. [22]:

$$f_i(x) = a_i\frac{1 + b_i(x + d_i)^2}{1 + c_i(x + e_i)^2}. \tag{4}$$

For a β-stable neutron star which consists of nucleons and leptons λ (e^- and μ^-), the Lagrangian density is similar to Eq. (1) except for adding a term for leptons.

The energy density and the pressure for neutron star matter are, respectively,

$$\begin{aligned}\varepsilon = &\sum_B \frac{2}{(2\pi)^3}\int_0^{k_{F_B}}\sqrt{k^2 + m_B^{*2}}dk^3 + \frac{1}{2}m_\sigma^2\sigma^2 \\ &+ \frac{1}{2}m_\omega\omega_0^2 + \frac{1}{2}m_\rho^2\rho_{0,3}^2 + \frac{1}{2}m_\delta^2\delta_3^2 \\ &+ \sum_\lambda \frac{2}{(2\pi)^3}\int_0^{k_{F_\lambda}}\sqrt{k^2 + m_\lambda^{*2}}dk^3. \end{aligned} \tag{5}$$

$$\begin{aligned}P = &\sum_B \frac{1}{3}\frac{2}{(2\pi)^3}\int_0^{k_{F_B}}\frac{k^2}{\sqrt{k^2 + m_B^{*2}}}dk^3 - \frac{1}{2}m_\sigma^2\sigma^2 \\ &+ \frac{1}{2}m_\omega^2\omega_0^2 + \frac{1}{2}m_\rho^2\rho_{0,3}^2 - \frac{1}{2}m_\delta^2\delta_3^2 + \rho\Sigma_0^R \\ &+ \sum_\lambda \frac{1}{3}\frac{2}{(2\pi)^3}\int_0^{k_{F_\lambda}}\frac{k^2}{\sqrt{k^2 + m_\lambda^{*2}}}dk^3. \end{aligned} \tag{6}$$

The structure equations of a static spherically symmetric relativistic star are the Tolman-Oppenheimer-Volkov (TOV) equations [27,28]:

$$\frac{dP}{dr} = -\frac{[P(r) + \varepsilon(r)][M(r) + 4\pi r^3P(r)]}{r[r - 2M(r)]}, \tag{7}$$

$$M(r) = 4\pi\int_0^R \varepsilon(r)r^2dr, \tag{8}$$

where $\varepsilon(r)$, $P(r)$ are the energy density and pressure of the star at radius r, respectively, and $M(r)$ is the total star mass inside a sphere of radius r. Taking the boundary conditions, $P(R) = 0$, $M(0) = 0$, one can calculate $P(r)$ and $M(r)$ taking the central density $\rho(0)$ as a single parameter. The point R defines the radius of the star, and the corresponding $M(R)$ is the gravitational mass.

III. RESULTS AND DISCUSSION

In this paper, the properties of nuclear matter and neutron stars are studied in density-dependent relativistic mean field with the effective interactions DD-MEδ which takes the δ meson into account. For comparison, the results calculated by DDRMF with DD-ME2, TW99, and PKDD interactions without the δ meson which have been studied systematically in Refs. [29,30] are also discussed. Table I shows the bulk quantities (i.e., the saturation density ρ_0, the binding energy per particle E_B/A, the incompressibility K, the symmetry energy

TABLE I. The saturation properties of nuclear matter for different effective interactions, including binding energy per particle E_B/A (MeV), incompressibility K (MeV), asymmetry energy coefficient $E_{\rm sym}$ (MeV), and the effective mass M^*/M.

	ρ_0(fm^{-3})	E_B/A	K	$E_{\rm sym}$	M^*/M
DD-MEδ	0.152	−16.12	219.1	32.35	0.609
DD-ME2	0.152	−16.14	251.1	32.30	0.572
TW99	0.153	−16.25	240.2	32.77	0.555
PKDD	0.150	−16.27	262.2	36.86	0.570

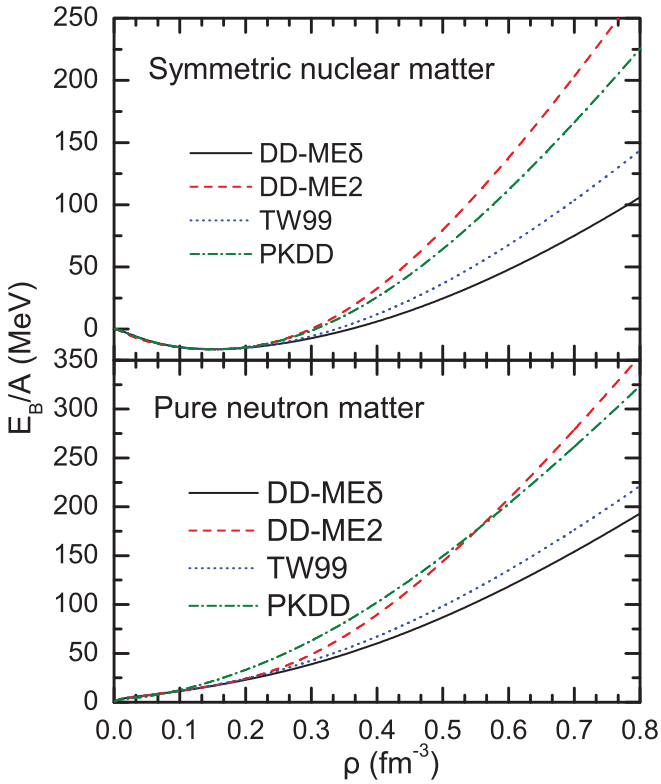

FIG. 1. (Color online) The binding energy per nucleon E_B/A, as a function of the nucleon density ρ for symmetric nuclear matter (upper panel) and pure neutron matter (lower panel). The results are calculated by DD-ME2, TW99, PKDD without the isovector scalar meson δ and DD-MEδ with the δ meson.

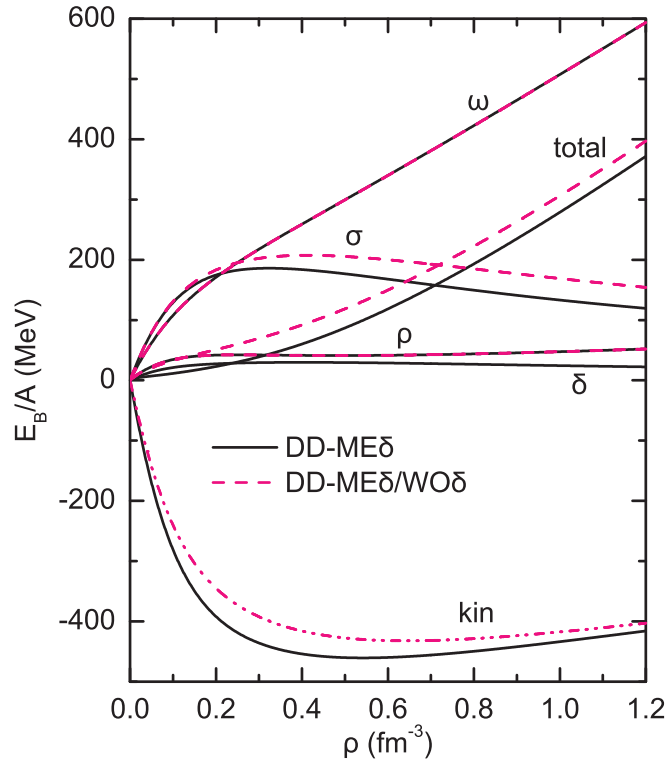

FIG. 2. (Color online) The contributions from different channels to the E_B/A as functions of the nucleon density ρ for the pure neutron matter. The results calculated by DD-MEδ (solid black lines) and DD-MEδ (dashed pink lines) but switching off the δ channel.

$E_{\rm sym}$, and the effective mass M^*/M) of symmetric nuclear matter at saturation point. It should be pointed out that the parameter set DD-MEδ fitted by the properties of finite nuclei and nuclear matter simultaneously around the saturation point with DD-ME2 as a starting point [22]. From the table we can see that the bulk properties of nuclear matter at saturation point calculated by DD-MEδ are very similar to DD-ME2 except for the incompressibility K. In all the interactions, DD-MEδ provides the smallest value of K, which is consistent with the empirical value $K \approx 230$ MeV [31]. For the symmetry energy $E_{\rm sym}$, PKDD obtains a larger value than the other interactions which give almost the same values. For the effective mass M^*/M, DD-MEδ gives the largest value and TW99 gives the smallest one.

The equations of state calculated by DD-MEδ are shown in Fig. 1 for symmetric nuclear matter (upper panel) and pure neutron matter (lower panel). The results calculated by density-dependent interactions without δ meson are also shown in the figure. As shown in Fig. 1, there are significant differences in the behaviors of the EOS in the high-density region for both the symmetric and pure neutron nuclear matter. For the symmetric nuclear matter in the upper panel of Fig. 1, among the interactions without the δ meson, DD-ME2 provides the hardest EOS and TW99 provides the softest. Meanwhile, the interaction DD-MEδ with the isovector scalar channel, obtains an even softer EOS than TW99. For the pure neutron matter in the lower panel of Fig. 1, it gives the same results as the situation for the symmetric nuclear matter, i.e., DD-MEδ still provides the softest EOS, and the EOS given by TW99 is a little stiffer than that by DD-MEδ.

To understand how the isovector scalar meson δ affects the EOS for the nuclear matter, the results calculated by DD-MEδ and DD-MEδ but switching off the isovector scalar channel will be compared in the following. The expression of the binding energy per nucleon E_B/A in the nuclear matter is similar to Eq. (5), and one can obtain the contributions from different channels to the E_B/A as

$$E_B/A = E_{B,\rm kin}/A + \sum_{\phi} E_{B,\phi}/A, \qquad (9)$$

where $\phi = \sigma, \omega, \rho$, and δ. In Fig. 2, the contributions from different channels to the E_B/A calculated by DD-MEδ and DD-MEδ but switching off the δ channel are shown as functions of the nucleon density ρ for the pure neutron matter. The total lines denote the binding energy per nucleon, and the others denote the contributions from different channels in the figure. Compared to the total E_B/A values, it is shown that the EOS becomes softer when the isovector scalar meson δ is taken into account. One can easily find that the introduction of the δ has no effect on the ω and ρ fields from the equations of different meson fields. Thus, as shown in Fig. 2, the contributions from ω and ρ parts are identical before and after switching off the δ channel, while the ones from both

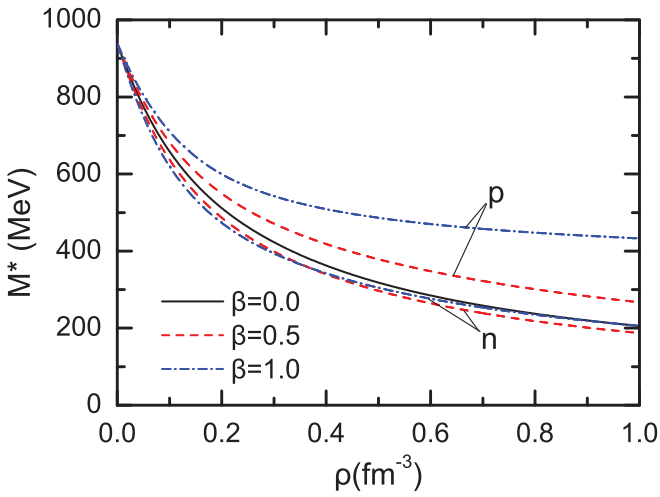

FIG. 3. (Color online) Neutron and proton effective masses as a function of the nucleon density with three different β.

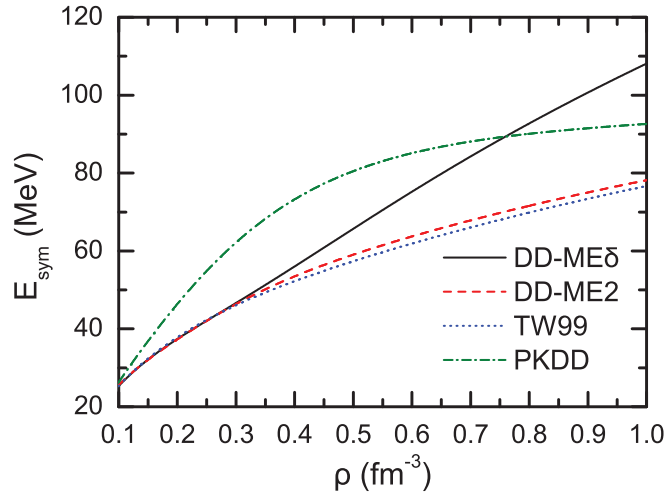

FIG. 4. (Color online) The nuclear matter symmetry energy $E_{\rm sym}$(MeV) as a function of the nucleon density ρ(fm^{-3}).

the kinetic part and the σ part calculated by DD-MEδ are smaller than the results by switching off the δ channel. For DD-MEδ, the δ channel has an extra contribution compared to the case of switching off the δ channel, however, such a contribution is very much smaller than the reductions of the contributions from the kinetic and the σ channel both affected by the δ channel. As a consequence, the contained isovector scalar δ channel can soften the EOS of nuclear matter.

When the isovector scalar δ meson is introduced, an interesting and important result, the n,p effective-mass splitting in asymmetric matter is obtained,

$$M_p^* = M - g_\sigma\sigma - g_\delta\delta_{0,3}, \tag{10}$$

$$M_n^* = M - g_\sigma\sigma + g_\delta\delta_{0,3}. \tag{11}$$

Figure 3 shows the proton and neutron effective masses for three different β values, calculated by DD-MEδ with increasing nuclear density. For the situation of $\beta = 0$, namely the symmetric nuclear matter, the proton effective mass obviously equals the neutron one and both of them become smaller as the density is increasing, as is shown in the figure. When the value of β deviates from 0, the effective mass splitting between the proton and the neutron and the results of $\beta = 0.5$ and $\beta = 1.0$ are also displayed in the figure. From Fig. 3, we can also see that the proton effective mass is larger than the neutron effective mass and the $M_p^* - M_n^*$ values are more and larger with the density increasing. For the widely used versions without the isovector scalar channel in RMF, the effective mass splitting vanishes. By the way, because the contributions to the isovector scalar channel from the Fock terms have an effect on the self-energies, it is conceivable that RHF calculations can also present the effective mass splitting. The result by the localization RHF is in agreement with the microscopic Dirac-Brueckner-Hartree-Fock (DBHF) result [32], which is used to provide directly the effective Dirac masses for the DD-MEδ parameter fit, namely, the effective mass splitting leading to the isovector scalar channel included by the Fock terms in RHF is similar to that leading to the δ meson in DD-MEδ.

In general, the energy per particle of asymmetric nuclear matter $E(\rho_b, \beta)$ can be expanded in the Taylor series with respect to the asymmetry parameter $\beta = (\rho_n - \rho_p)/(\rho_n + \rho_p)$,

$$E(\rho_0,\beta) = E_0(\rho_b) + \beta^2 E_{\rm sym}(\rho_b) + \cdots. \tag{12}$$

The function $E_0(\rho_b)$ is the binding energy per particle in symmetric nuclear matter. The symmetry energy $E_{\rm sym}(\rho_b)$ is denoted as

$$E_{\rm sym}(\rho_b) = \frac{1}{2}\frac{\partial^2 E(\rho_b,\beta)}{\partial\beta^2}\bigg|_{\beta=0}. \tag{13}$$

The symmetry energy is an important quantity for illustrating the property of asymmetric nuclear matter. The value of the symmetry energy at the symmetric nuclear matter saturation density is known to be around 32 MeV. However, the density dependence of the symmetry energy at the high-density region is quite divergent [33–35].

Figure 4 shows the symmetry energy as a function of the baryon density ρ_b with different effective interactions. It is conceivable that the δ meson, as an isovector meson, impacts the symmetry energy of nuclear matter. As shown in Fig. 4, the symmetry energy behavior obtained by DD-MEδ is obviously different from those by the interactions without the δ meson. Among the calculations of the effective interactions without the δ meson, PKDD exhibits a stiffer symmetry energy behavior than DD-ME2 and TW99, both of which show similar symmetry energy in the whole density region. The contribution of the δ meson to the symmetry energy is negative essentially, while to keep the symmetry energy at saturation density, the enhanced rho coupling leads to stiffer density-dependent behavior at the height density region [36]. The final result is a strong density dependence of the symmetry energy under the joint actions of the δ coupling and ρ coupling. The different contributions to the symmetry energy are displayed in Ref. [22]. By the way, the Fock terms in the RHF calculations also enhance the density dependence of the symmetry energy and the detailed investigation was shown in Ref. [30]. For the RHF calculations, all the meson nucleon couplings present a

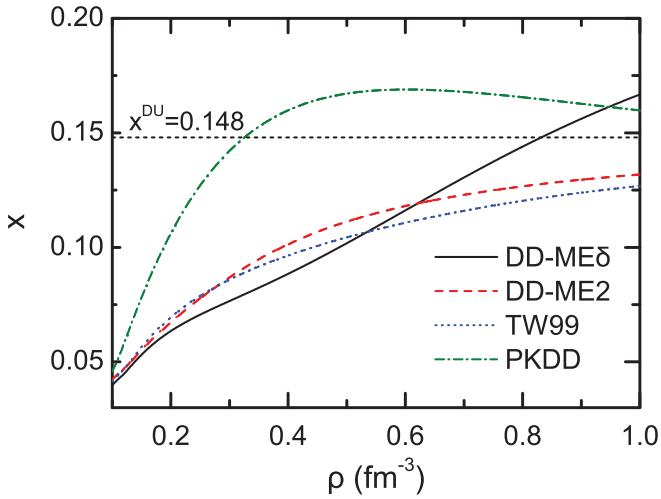

FIG. 5. (Color online) Proton fractions $x = \rho_p/(\rho_p + \rho_n)$ in neutron star given by different effective interactions. The dotted line labeled with $x^{\rm DU} = 14.8\%$ is the threshold for the direct Urca process to occur.

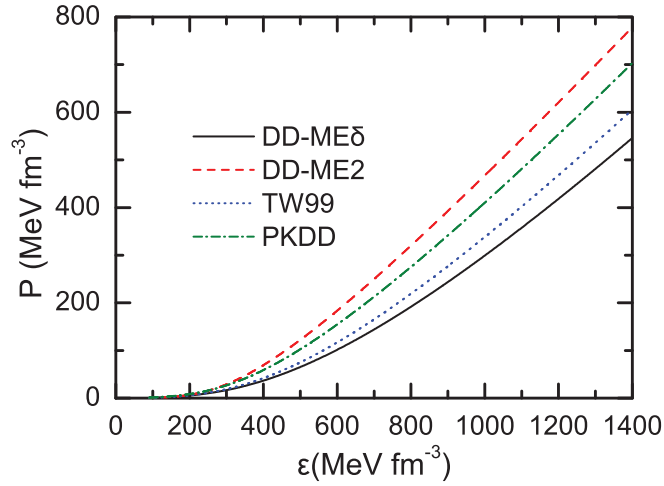

FIG. 6. (Color online) The pressure of neutron star matter as a function of the energy density ε (MeV fm^{-3}).

significant contribution to the symmetry energy from the Fock terms, which results in the enhancement.

It is known that the nuclear matter symmetry energy is namely the energy required per particle to change the symmetric nuclear matter into the pure neutron matter. Thus, the stronger density dependence of the symmetry energy at the high-density region means that it is more difficult for the system to become asymmetric and it is easier for the neutrons to β decay which gives rise to greater proton abundance.

We now turn to the properties of neutron stars. Figure 5 shows the proton fraction x as a function of nucleon density ρ calculated by DD-MEδ in comparison to those effective interactions neglecting the isovector scalar channel. As mentioned above, the curves for the proton fraction are similar to the trends of the symmetry energy (see Figs. 4 and 5) accounting for the influence of the symmetry energy on the proton abundance. Because of the stiff symmetry energy, a somewhat strong density dependence of the proton fraction is obtained by PKDD. For the DD-MEδ, the curve of the proton fraction still intersects with the one by PKDD, and gets stiffer than that by DD-ME2. In Fig. 4, the density dependence of the symmetry energy obtained by DD-ME2 and TW99 are similar with each other in the entire density region, and this behavior also demonstrates in Fig. 5 the proton fraction.

The proton fraction affects the cooling mechanism of neutron stars directly, namely, it determines whether the most efficient process of the neutron star cooling (the so-called direct Urca process [37]) could take place or not. Direct Urca (DU) processes $n \to p + e^- + \bar{\nu}_e$ and $p + e^- \to n + \nu_e$ lead the star to cool rapidly by emitting thermal neutrinos. The threshold of the proton fraction $x^{\rm DU}$ for triggering the DU process is constrained in the region of 11.1%–14.8% [38,39]. Because of the muon presence, the threshold $x \approx 14.8\%$ is more reasonable in the high-density region [39]. From Fig. 5, it is found that the proton fraction given by DD-MEδ and PKDD can exceed the threshold $x^{\rm DU}$ and may be in favor of undergoing the DU process, whereas the results given by DD-ME2 and TW99 are below the threshold $x^{\rm DU}$ and do not support the occurrence of DU progress. The critical densities $\rho^{\rm DU}$ for the DU process occurring obtained by DD-MEδ and PKDD are 0.83 and 0.33, respectively. The critical mass $M^{\rm DU}$ and central density values $\rho^{\rm DU}(0)$ where the DU cooling process becomes possible are marked by the filled squares in Fig. 7.

Figure 6 shows the calculated pressure of neutron star matter as a function of the energy density ε (MeV fm^{-3}). The results for the neutron star matter are the same as those for the nuclear matter, of which the EOS is obviously softened by DD-MEδ when considering the δ meson. It is known that the isovector scalar meson δ contributes an attractive field which reduces the system repulsion, and thus the inclusion of the δ meson will lead to a larger proton fraction, and consequently cause a smaller symmetry repulsion. EOS, as the input of the TOV equation, significantly affects the mass-radius relation of the neutron stars. A stronger density dependence of the pressure at high densities would deduce a larger maximum mass for neutron stars that can be sustained against collapse. By the way, because the relativistic mean field theory is not suitable to be used when the density is below 0.09 fm^{-3}, the BPS [40] and BBP [41] models are chosen to provide the proper EOS.

Figure 7 displays the neutron star masses as a function of the central density $\rho(0)$ of the star, with several effective interactions mentioned above. From Fig. 7, it can be seen that DD-MEδ exhibits the smallest maximum mass at the largest central density $\rho_{\rm max}(0) = 1.20$ fm^{-3}. Table II shows the maximum mass limits $M_{\rm max}$ and the corresponding central densities $\rho_{\rm max}(0)$ extracted from Fig. 7.

The filled squares denote the critical mass $M^{\rm DU}$ and central density values $\rho^{\rm DU}(0)$ where the DU cooling process becomes possible. The critical masses $M^{\rm DU}$ are 1.86 $M_\odot$ and 1.28 $M_\odot$ for DD-MEδ and PKDD, respectively. According to the analysis in Refs. [39,42,43], if the DU process is taken as a possible mechanism for neutron star cooling, an acceptable EOS would not allow it to occur in typical neutron stars which

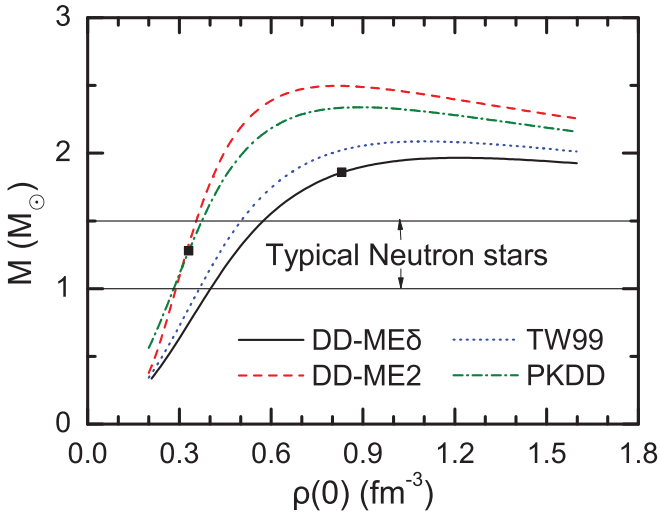

FIG. 7. (Color online) Neutron star mass as a function of the central density for different effective interactions. The filled squares mark the critical mass $M^{\rm DU}$ and central density values $\rho^{\rm DU}(0)$ where the DU cooling process becomes possible. The mass region of typical neutron stars is between $1.0M_{\odot}$ and $1.5M_{\odot}$.

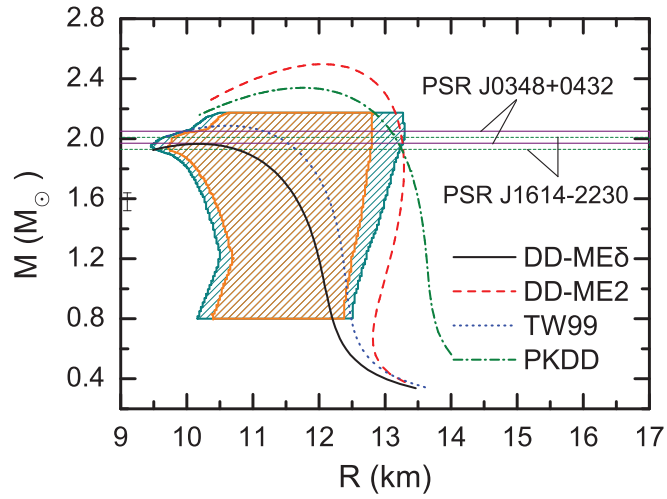

FIG. 8. (Color online) Mass radius of neutron stars calculated by the interactions without the δ meson and the interaction DD-MEδ with the δ meson. The two shaded areas are 68% and 95% confidence contours extracted from the analysis of Ref. [11].

have masses in the range of 1.0 $M_{\odot}$–1.5 $M_{\odot}$. From Fig. 7, it is obvious that the mass limit $M_{\rm DU}$ given by PKDD is too small to satisfy the principle that the DU process shall not occur in typical neutron stars. In contrast, DD-MEδ gives a mass limit $M_{\rm DU}$ above 1.5 $M_{\odot}$, perfectly supporting the DU process. In conclusion, the density dependence of the symmetry energy is too strong for PKDD and too weak for DD-ME2, TW99 to support the DU process, while only the effective interaction DD-MEδ provides a proper symmetry energy behavior for the DU process constraint.

Figure 8 shows the calculated mass-radius relations of neutron stars. Consistent with the EOSs in Fig. 6, the maximum mass of the neutron star and the corresponding radius given by DD-MEδ are the smallest, and those obtained by DD-ME2 are the largest. The results for TW99 are similar to DD-MEδ but its calculations for both mass and radius are a little larger than DD-MEδ.

It is usually considered that the radius of the neutron star is sensitive to the density dependence of the symmetry energy, and the stiffer symmetry energy is related to a larger size of the neutron star [34,44,45]. Reference [46] displays the correlation coefficients between the radius of a 1.4 $M_{\odot}$ neutron star $R_{1.4}$ and slope of the symmetry energy L as well as the symmetry energy. But $R_{1.4}$ cannot be uniquely constrained by the symmetry energy, and actually the radius $R_{1.4}$ is extremely sensitive to the equation of state at high density [44], which can be clearly found in Fig. 8. Although DD-MEδ provides the strong symmetry energy behavior, the calculated radius of the neutron stars still remains somewhat small owing to the soft EOS.

The shadow regions in Fig. 8 show the 68% and 95% confidence contours for the mass-radius relation predicted by Steiner [11]. This reference shows that the radius of a 1.4 solar mass neutron star lies between 11.2 and 12.3 km. As shown in Fig. 8, the mass-radius relation for the neutron stars given by DD-MEδ with the δ meson totally covers the constraints. Among the interactions without the δ meson, because of a little stiffer EOS at the density region, DD-ME2 and PKDD hardly cover the constraints, while TW99 fulfills the constraints. Table II shows the maximum mass limits $M_{\rm max}$, the corresponding radii $R(M_{\rm max})$, and the radii $R_{1.4}$ for $1.4M_{\odot}$ extracted from Fig. 8. It is shown that the maximum mass calculated by DD-MEδ is exactly the same as the heaviest neutron stars observed currently which are PSR J1614 − 2230 with $1.97 \pm 0.04\ M_{\odot}$ [4] and PSR J0348 + 0432 with $2.01 \pm 0.04\ M_{\odot}$ [5], respectively. The radius for the 1.4 solar mass neutron star obtained by DD-MEδ and TW99 are consistent with the prediction in Ref. [11], while the results for DD-ME2 and PKDD are not. The consistency between the maximum mass and the radius of the neutron star with the recent observations reflects that the EOS and the density dependence of the symmetry energy given by DD-MEδ seem proper to describe the properties of neutron stars.

TABLE II. Maximum mass $M_{\rm max}(M_{\odot})$, and the corresponding central densities $\rho_{\rm max}(0)({\rm fm}^{-3})$ and radii $R(M_{\odot})$(km), and the radii (km) for $1.4M_{\odot}$ neutron stars.

	DD-MEδ	DD-ME2	TW99	PKDD
$M_{\rm max}$	1.97	2.50	2.09	2.34
$\rho_{\rm max}(0)$	1.20	0.82	1.10	0.89
$R(M_{\rm max})$	10.2	12.0	10.6	11.8
$R(1.4M_{\odot})$	11.9	13.1	12.3	13.6

IV. SUMMARY

In this paper, we studied the general properties of nuclear matter and neutron stars based on the density-dependent relativistic mean field theory with the interaction DD-MEδ. It is shown that the inclusion of the isovector scalar meson

δ, obviously affects the symmetry energy behavior of the nuclear matter, which is a stronger density dependence of the symmetry energy obtained by DD-MEδ. Therefore, the proton fraction $x = \rho_p/(\rho_p + \rho_n)$ of the neutron star is also enhanced owing to introducing the δ meson, which affects essentially the cooling process of the star. For the DU process to occur, DD-MEδ gives the critical density $\rho^{\mathrm{DU}} = 0.83\ \mathrm{fm}^{-3}$ and the critical mass $M^{\mathrm{DU}} = 1.86 M_{\odot}$; DD-ME2 and TW99 do not support the DU progress occurring in the neutron star; PKDD can give the proton fraction exceeding the threshold of the proton fraction x^{DU} for the DU process occurrence, but gives the critical mass $M^{\mathrm{DU}} = 1.28 M_{\odot}$, which violates the assumption that the DU process shall not occur in typical neutron stars. In a word, DD-MEδ provides a proper symmetry energy behavior for the DU process constraint.

By comparing with the results calculated by DD-MEδ but switching off the δ channel, it is concluded that the isovector scalar channel softens the EOS for the nuclear matter owing to the reduction of the contributions from the kinetic and the σ parts. It is shown that DD-MEδ provides the softest EOS for neutron star matter in the selected effective interactions, thus leading to the largest central densities of the neutron stars. Based on this EOS, DD-MEδ presents the smaller neutron star mass and radius. In all the selected interactions, DD-MEδ gives a quite small radius which is in good agreement with the recent observations according to Ref. [11], while the DD-ME2 and PKDD are not. The maximum mass given by DD-MEδ also agrees with the two heaviest neutron stars observed currently. In conclusion, the perfect consistency between the maximum mass and the radius of the neutron star with the recent observations reflects that the EOS predicted by DD-MEδ is suitable to describe the properties of neutron stars.

ACKNOWLEDGMENTS

We would like to thank W. H. Long and B. Y. Sun for helpful discussions. The work is supported by the National Natural Science Foundation of China (Grant No. 11175074) and the Fundamental Research Funds for the Central Universities (Grant No. lzujbky-2012-5).

[1] J. Lattimer and M. Prakash, Science **304**, 536 (2004).
[2] L. D. Landau, Phys. Z. Sowjetunion **1**, 285 (1932).
[3] W. H. Long, B. Y. Sun, K. Hagino, and H. Sagawa, Phys. Rev. C **85**, 025806 (2012).
[4] P. Demorest, T. Pennucci, S. Ransom, M. Roberts, and J. Hessels, Nature (London) **467**, 1081 (2010).
[5] J. Antoniadis, P. C. Freire, N. Wex, T. M. Tauris, R. S. Lynch, M. H. van Kerkwijk, M. Kramer, C. Bassa, V. S. Dhillon, T. Driebe *et al.*, Science **340**, 1233232 (2013).
[6] J. S. Read, B. D. Lackey, B. J. Owen, and J. L. Friedman, Phys. Rev. D **79**, 124032 (2009).
[7] F. Özel, G. Baym, and T. Güver, Phys. Rev. D **82**, 101301 (2010).
[8] A. W. Steiner, J. M. Lattimer, and E. F. Brown, Astrophys. J. **722**, 33 (2010).
[9] A. W. Steiner and S. Gandolfi, Phys. Rev. Lett. **108**, 081102 (2012).
[10] K. Hebeler, J. M. Lattimer, C. J. Pethick, and A. Schwenk, Phys. Rev. Lett. **105**, 161102 (2010).
[11] A. W. Steiner, J. M. Lattimer, and E. F. Brown, Astrophys. J. Lett. **765**, L5 (2013).
[12] B. D. Serot and J. D. Walecka, Adv. Nucl. Phys. **16**, 1 (1986).
[13] P.-G. Reinhard, Rep. Prog. Phys. **52**, 439 (1989).
[14] P. Ring, Prog. Part. Nucl. Phys. **37**, 193 (1996).
[15] J. Meng, H. Toki, S.-G. Zhou, S. Zhang, W. Long, and L. Geng, Prog. Part. Nucl. Phys. **57**, 470 (2006).
[16] S. Kubis and M. Kutschera, Phys. Lett. B **399**, 191 (1997).
[17] B. Liu, V. Greco, V. Baran, M. Colonna, and M. Di Toro, Phys. Rev. C **65**, 045201 (2002).
[18] V. Greco, M. Colonna, M. Di Toro, and F. Matera, Phys. Rev. C **67**, 015203 (2003).
[19] T. Gaitanos, M. Di Toro, S. Typel, V. Baran, C. Fuchs, V. Greco, and H. Wolter, Nucl. Phys. A **732**, 24 (2004).
[20] D. P. Menezes and C. Providência, Phys. Rev. C **70**, 058801 (2004).
[21] B. Liu, H. Guo, M. Di Toro, and V. Greco, Eur. Phys. J. A - Hadrons and Nuclei **25**, 293 (2005).
[22] X. Roca-Maza, X. Vinas, M. Centelles, P. Ring, and P. Schuck, Phys. Rev. C **84**, 054309 (2011).
[23] H. Liang, P. Zhao, P. Ring, X. Roca-Maza, and J. Meng, Phys. Rev. C **86**, 021302(R) (2012).
[24] G. A. Lalazissis, T. Nikšić, D. Vretenar, and P. Ring, Phys. Rev. C **71**, 024312 (2005).
[25] S. Typel and H. Wolter, Nucl. Phys. A **656**, 331 (1999).
[26] W. Long, J. Meng, N. Van Giai, and S.-G. Zhou, Phys. Rev. C **69**, 034319 (2004).
[27] R. C. Tolman, Phys. Rev. **55**, 364 (1939).
[28] J. R. Oppenheimer and G. M. Volkoff, Phys. Rev. **55**, 374 (1939).
[29] S. F. Ban, J. Li, S. Q. Zhang, H. Y. Jia, J. P. Sang, and J. Meng, Phys. Rev. C **69**, 045805 (2004).
[30] B. Y. Sun, W. H. Long, J. Meng, and U. Lombardo, Phys. Rev. C **78**, 065805 (2008).
[31] J. Piekarewicz, Phys. Rev. C **76**, 031301 (2007).
[32] E. N. E. van Dalen, C. Fuchs, and A. Faessler, Eur. Phys. J. A **31**, 29 (2007).
[33] V. Baran, M. Colonna, V. Greco, and M. Di Toro, Phys. Rep. **410**, 335 (2005).
[34] A. W. Steiner, M. Prakash, J. M. Lattimer, and P. J. Ellis, Phys. Rep. **411**, 325 (2005).
[35] B.-A. Li, L.-W. Chen, and C. M. Ko, Phys. Rep. **464**, 113 (2008).
[36] B. Liu, M. Di Toro, V. Greco, C. W. Shen, E. G. Zhao, and B. X. Sun, Phys. Rev. C **75**, 048801 (2007).
[37] C. Pethick, Rev. Mod. Phys. **64**, 1133 (1992).
[38] J. M. Lattimer, C. J. Pethick, M. Prakash, and P. Haensel, Phys. Rev. Lett. **66**, 2701 (1991).
[39] T. Klähn, D. Blaschke, S. Typel, E. Van Dalen, A. Faessler, C. Fuchs, T. Gaitanos, H. Grigorian, A. Ho, E. Kolomeitsev *et al.*, Phys. Rev. C **74**, 035802 (2006).
[40] G. Baym, C. Pethick, and P. Sutherland, Astrophys. J. **170**, 299 (1971).

[41] G. Baym, H. A. Bethe, and C. J. Pethick, Nucl. Phys. A **175**, 225 (1971).
[42] D. Blaschke, H. Grigorian, and D. N. Voskresensky, Astron. Astrophys. **424**, 979 (2004).
[43] S. Popov, H. Grigorian, R. Turolla, and D. Blaschke, Astron. Astrophys. **448**, 327 (2006).
[44] C. J. Horowitz and J. Piekarewicz, Phys. Rev. C **64**, 062802 (2001).
[45] C. J. Horowitz and J. Piekarewicz, Phys. Rev. Lett. **86**, 5647 (2001).
[46] F. J. Fattoyev and J. Piekarewicz, Phys. Rev. C **84**, 064302 (2011).